ANALYSIS OF A SINGLE SUBSONIC JET INTERACTING WITH A FLAT PLATE

Odenir de Almeida, odenir@mecanica.ufu.br
Tiago de Assis Silva, tasilva@mecanica.ufu.br
Aristeu da Silveira Neto, aristeus@mecanica.ufu.br
Federal University of Uberlândia – UFU, Brazil

Abstract. *The present work describes a preliminary numerical study of a single subsonic jet interacting with a flat plate immersed into the flow. Such study is part of an ongoing research about jets interacting with surfaces as seen in powerplant installations for aircrafts.The main goal of this research is to develop means of predicting the flowfield and acoustics of a jet interacting with pylons and wings. Before achieving such task, a step back is given in order to analyse the flowdynamics of a single jet interacting with a flat plate mainly due to the difficulty of finding in the open literature fundamental works describing the main parameters that governates such phenomenon and its correlations with the generated noise. By considering this, in order to analysis the flowdynamics and later on the aerocoustics of these interactions a set of CFD and CAA (Computational Aeroacoustics) tools have been applied for a simple configuration. Some insights about the acoustics have been taken considering a previous experimental work. The observations and results collected in this work serve as background for a more challenging phase towards the prediction of a more complex configuration.*

Keywords*: Aeroacoustics, Subsonic Jet, Flat Plate, Powerplants, Engine Noise.*

1. INTRODUCTION

The propulsive integration is a very challenging problem in the aircraft design process. At early stages of designing the aircraft the engines must be considered to be placed under different configurations: a) under wing; b) rear-mounted and c) over-mounted. The choice of the configuration will impact the aircraft aerodynamics, weight, vibration, engine performance, maintenance and specially noise [1], mainly due to interactions of the jet with surfaces as pylons and flaps. All these parameters must be addressed in order to lead to a clean and efficient configuration. Regarding noise, there is no more doubt that this is one of the most important design parameters and must be analyzed either through numerical methods or experimental techniques. However, one very important question arises: How to evaluate the noise at early stages of an aircraft design?

In the last years the academic and industrial attention has been diverted in developing methods to answer this question. Experimental techniques have been used as a complementary tool to provide baseline database, however the most important development can be seen in the numerical area. This could not be so different since the cost involved with experimental techniques is also prohibitive in several aspects. In order to reduce noise from modern aircrafts, it is important to understand the mechanisms of sound generation and propagation for each aircraft component including situations where there is interaction of one source with another. At this point, it is important to draw the attention to the engines specifically since they are the most important contributors to noise in modern's aircraft, particularly during takeoff. The fan and jet are the most significant noise sources and have been the focus of the majority of engine noise research in recent years. The aircraft powerplant produces most of the noise heard on the ground and within the passenger cabin, although the airframe may play an important role in shielding or amplifying such sources [2].

Despite the other noise sources in a modern turbofan engine, jet noise is largely dominant at take-off and still constitutes one of the biggest concerns in the aerospace industry. In order to reduce and/or quantify the jet noise and its interaction with pylons and flaps some attempts have been made relying on empirical database methods (normally from model rig data extrapolated to full scale) and by evolution of the past experience of engine and aircraft manufacturers. Many experiments were carried out trying to quantify the characteristics and intensity of installation noise [3], [4], [5] and [6], among others. These experiments were conducted in rigs involving measurements of the jet alone and also its interference with wings and flaps in an anechoic chamber. It is important to emphasize that many of these works generated proprietary information which are not shared in the open literature. This situation is commonly seen in this area and imposes a lot of restrictions to those looking at fundamental research.

A preliminary study has been performed in order to establish the basis for the simulations considering a jet flow interacting with a surface; in this case a flat plate placed downstream the nozzle exit plane. Some initial tests have been performed considering a simple 2D planar domain in order to check aspects like mesh generation and refinement as well as boundary conditions. It was identified some important aspects like the importance of mesh refinement in the region of the flat plate. Moreover, the preliminary results also indicate that the flow field may be severely influenced by the parameters L and H, length from the nozzle exit plane and height of the plate above the nozzle, respectively. The next step performed was a full 3D simulation. A complete set of numerical results are shown in this study. A step further will be the acoustic prediction, the main challenge of this ongoing research.

2. NUMERICAL APPROACH

As previously mentioned, this study is part of an ongoing research about the fluidynamics and acoustic of a subsonic jet interacting with surfaces placed in the flow like pylons and flaps. As discussed before such problem is very complex not only under the flow dynamics viewpoint but also when considering the sound produced by the turbulence generated as consequence from this interaction. Dealing numerically with this problem is also something challenging, mainly due to aspects as compressibility, turbulence, flow detachment and reattachment and aeroacoustics.

Considering all these facts together a strategy was considered in terms of numerical approach for this problem as can be listed below:

a) A preliminary comparison among some aerodynamic parameters from a single axissymmetric jet and a planar jet interacting with a flat plate was considered. For the *baseline* simulation the single jet was considered to be axissymmetric. For the jet interacting with a flat plate the simulations have been executed in a 2D domain framework as a complete planar jet. It is important to emphasize the reason for this approach. The idea was to check in a 2D framework the issues with the mesh generation and setting of boundary conditions, as well as to look generally to the flowfield in order to get some insights about it. It must be clear that from the flow dynamics point of view the axissymmetric and the 2D planar jets are obviously very different.
b) After getting knowledge about parameters like mesh generation, the next step was to build a complete tridimensional (3D) domain and to perform the numerical simulations. Two simulations have been performed, one without the presence of the flat plate (free single jet flow - *baseline*) and the other with the presence of the plate downstream the jet exit plane.

Details about the numerical methodology and computational code as well as geometric information and numerical model are presented in the next subsections. The numerical results of this work were compared with experimental data from Jordan *et al.* [7] for single jets and with data from Shearin [8] for a single jet interacting with a flate plate.

2.1. Numerical Method for Fluid Dynamics

In the present work, in order to run the 2D and 3D RANS simulations, the commercial CFD++ code was employed through a non-linear k–ε closure approach, named k–ε cubic model. The formulation to obtain the Reynolds-stress tensor is defined via a tensorial expansion, cubic in the mean strain and vorticity tensors. The stresses are related to the mean strain and vorticity using the quadratic model of Shih et al. [9] with the cubic extension proposed by Lien and Leschziner [10]. More details about the model are given in Goldberg et al. [11].

2.2. Nozzle Geometry

In order to perform the simulations, a nozzle with D = 50 mm, smooth contraction and sharp lip was used as a test bench for the jet flow noise measurements and aerodynamic numerical simulations. A general description of the geometry is depicted in Figure 1.

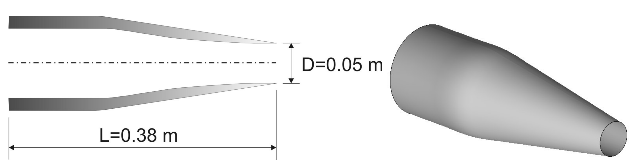

Figure 1. Nozzle geometry for single jet flow.

2.3. Flow Conditions

Table 1 presents the flow conditions for the single jet flow investigated in this work. These flow conditions were applied to all the simulations including the axissymmetric, planar tests and the full 3D jet interacting with a flat plate. The unheated jet is simulated, i.e. the static temperature in the nozzle exit plane, T_j , is equal to the static temperature of the ambient air, T_0 .

Table 1. Flow conditions – single jet.

Case	U_j / c_∞	T_j / T_0	U_j (m/s)	c_∞ (m/s)	P_j (Pa)	ρ_∞ (kg/m^3)	P_0 (Pa)	T_0 (K)
1	0.75	1.0	253.31	337.75	144400	1.225	99670	283.15

2.4. Computational Domains and Boundary Conditions

The dimensions for the computational domain used in the RANS simulations are illustrated in Figure 2 and 3. Even for the preliminary tests with both axissymmetric and planar jets the same size of domain was used. Again the size of the domain in x and y coordinates was selected after some cautious check out in the literature. The domain size was scaled based on the nozzle exhaust diameter D_j. The longitudinal size of the domain was set to 50 D_j with an outer boundary having a hyperbolic tangent like distribution along the axis direction such that the radial extend is 10 D_j at the nozzle inlet plane and 20 D_j at the domain outlet. A small flat plate was positioned just over the nozzle exhaust in such a way that a weak interaction with the shear layer will be expected. These interaction parameters have been selected from the work of Shearin [8].

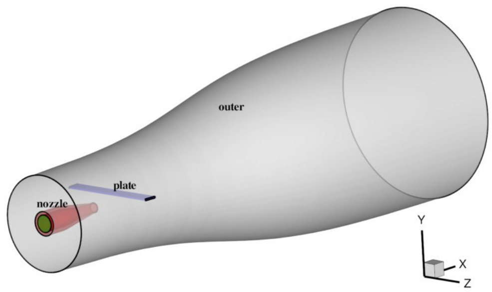

Figure 2. Schematic view of the 3D computational domain for single jet and jet plate interaction RANS simulations.

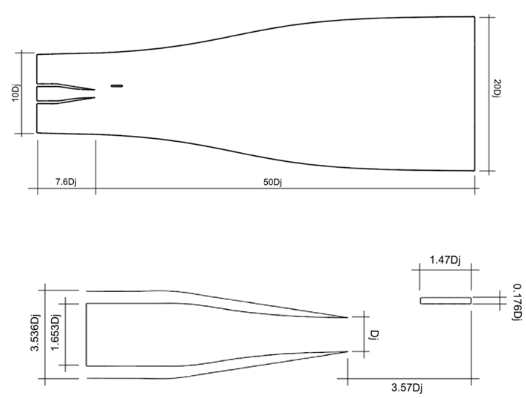

Figure 3. Extend of the computational domain based on jet diameter (D_j) – 3D jet flow.

Regarding boundary conditions, at the inlet of the nozzle, total pressure and total enthalpy are specified. All free boundaries, i.e. upstream (left) and entrainment boundary (upper), are defined using a static pressure at the outlet boundary. Yet, at the domain outlet (right) static pressure is also specified. Figure 4 summarizes the main boundary condition used in all simulations.

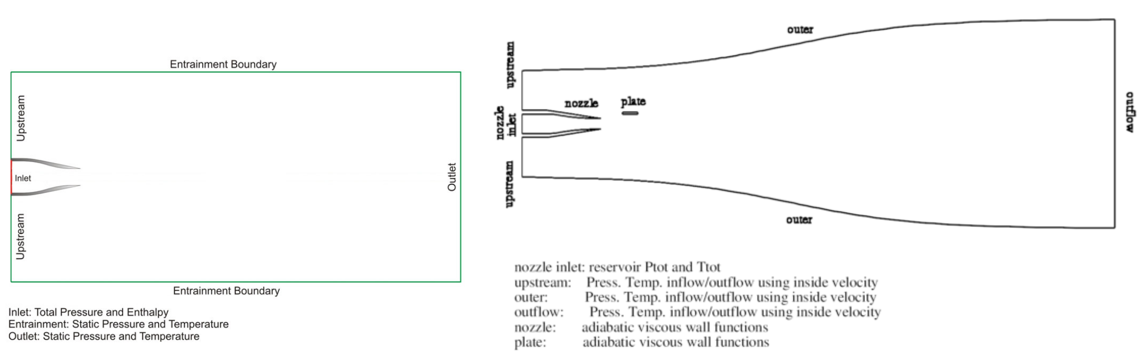

(a) (b)

Figure 4. Boundary conditions – (a) Planar Jet Flow; (b) Full 3D domain.

In the software CFD++ these boundary conditions are translated as:
Inlet: Reservoir Ptot Ttot (Stagnation Pressure and Temperature)
Entrainment Boundary: Pres. Temp. inflow/outflow using inside velocity
Upstream and Downstream: Pres. Temp. inflow/outflow using inside velocity
Nozzle: Adiabatic viscous wall function

For turbulence, the ratio of turbulent viscosity and molecular viscosity was set as 10 and at the inlet a level of approximately 10% of turbulence intensity was considered.

2.5. Numerical Scheme

In CFD++ the governing equations were solved with a second order accuracy through what is called Compressible PG Navier-Stokes/Euler system. The final solution was obtained by employing a cubic k-epsilon turbulence model running approximately 750 iterations with a residual decaying approximately 4 orders of magnitude.

2.6. Mesh Refinement

Five distinct domains were used in this work. The mesh refinement for each one is briefly described below.

a) Axissymmetric domain: The final axissymmetric computational domain discretization consisted of a block structured mesh with 8 blocks and a total of 124918 elements. The mesh points are concentrated to the shear layer region and clustered in the nozzle wall in order to provide a y^+ less than 20 in the near wall region. A geometric growing law is used to increase the elements in axial and radial direction. A sharper mesh jump is avoided during block transitions – Figure 5.

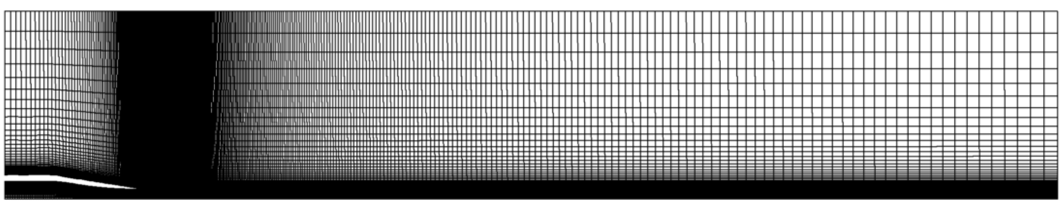

Figure 5. Mesh refinement – axissymmetric domain.

b) Planar (2D) domain with and without flat plate: The final 2D computational domain discretization consisted of block structured meshes with 19 blocks and a total of 113923 elements for the single jet flow interacting with a flat plate and 17 blocks and a total of 82672 elements for the single jet flow without the presence of the flat plate. The mesh points were concentrated to the shear layer region and clustered in the nozzle wall following a 7th-law turbulent boundary layer approach in order to provide a Y^+ of approximately 30 in the near wall regions. A linear growing law is used to increase the elements in axial and radial direction. A sharper mesh jump is avoided during block transitions – Figure 6.

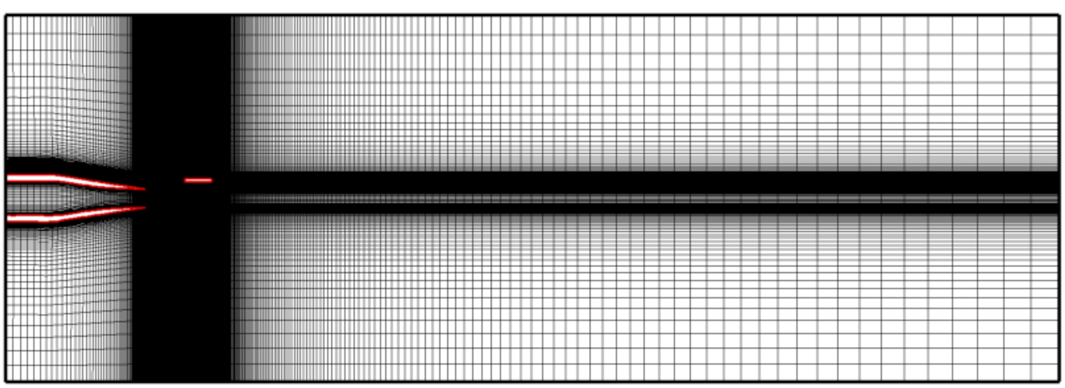

Figure 6. 2D planar domain with flat plate.

c) 3D domain with and without the plate: The final 3D computational domain discretization consisted of block structured meshes with 151 blocks and a total of 7714413 elements for the single jet flow interacting with a flat plate and 21 blocks and a total of 7074270 elements for the single jet flow without the presence of the flat plate. The mesh points were concentrated to the shear layer region and clustered in the nozzle wall in order to provide a y^+ of approximately 20 in the near nozzle wall regions. A geometric growing law is used to increase the elements in axial and radial direction. A sharper mesh jump is avoided during block transitions. In order to mesh the computational domains using hexahedron elements, a multiblock like structure was used for the single jet and jet plate computational domains – Figure 7. The reason for such size of mesh was the number of points used to discretize the shear-layer region, as can be seen in Figure 7.

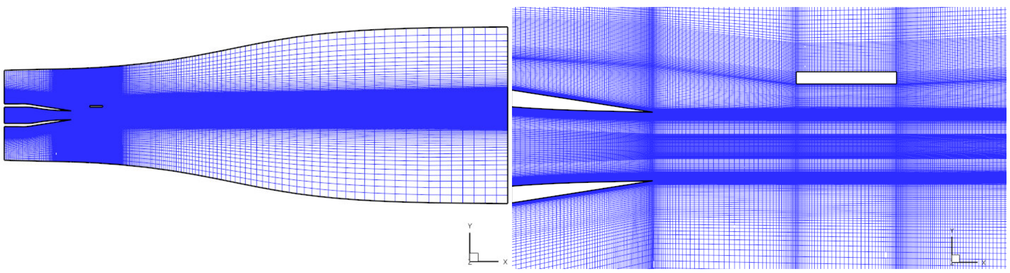

(a) Mesh refinement along plane xy for jet plate computational domain.

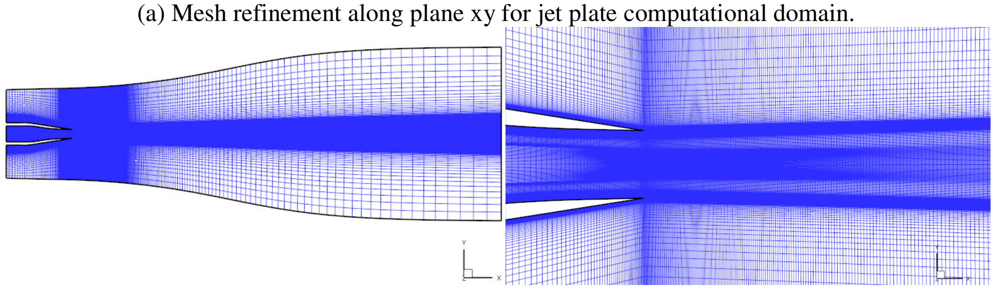

(b) Mesh refinement along plane xy for single jet computational domain.

Figure 7. Mesh refinement – (a) jet/plate; (b) single jet - *baseline*.

3. NUMERICAL RESULTS

The numerical results from all simulations performed in this work are presented in the next subsections, considering each set of tests.

3.1. Axissymmetric Jet - Validation

The axissymmetric jet simulations were considered in order to validate a single free jet flow operating in the subsonic regime at Mach number equal to 0.75. It is important to point out that this first test was dedicated to a more detailed study about the aerodynamics of the single jet flow. Despite the fact that some results have been previously presented in Almeida [2], the idea here was to include more parameters for validation like the stress tensor's components. By doing that, it is possible to have more confidence in the numerical model employed in CFD++ and consequently in the aerodynamic results.

The aerodynamics results presented herein includes velocity distribution and stress tensor's components in the jet centerline and also radial profiles in three different axial positions downstream of the nozzle exit according to Figure 8. The numerical results shown here were obtained with an axissymmetric and a 3D mesh. The numerical results were validated using the data of Jordan *et al.* [7].

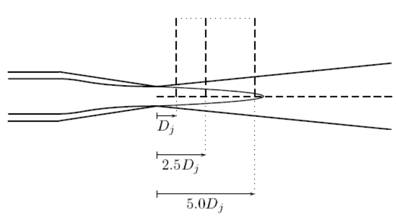

Figure 8. Profiles of axial velocity and second-order moments are obtained along de centerline and along three radial lines.

Figure 9 shows a set of different aerodynamics results including velocity distribution and Reynolds stress tensor components at axial and radial positions. The main observations can be listed as below:

1) In all predicted flow fields the initial mixing is underpredicted, resulting in a longer potential core length. Besides that, the numerical results obtained with CFD++ indicate a more accentuated decay rate when compared with experimental results. In the literature such behavior is generally related to the presence of numerical dissipation in the schemes.
2) The peak levels of predicted turbulence intensity are shifted downstream of the nozzle exit, which is consistent with the overprediction of potential core lengths since the maximum turbulence intensity is found where the potential core vanishes. The shape and the peak levels of predicted turbulence intensities, calculated from the anisotropic cubic k-ε turbulent model, were very close to the experimental data.
3) Even though the RANS simulations fail to predict the potential core length, the cross-section axial velocity distribution shows a good agreement with experimental data.

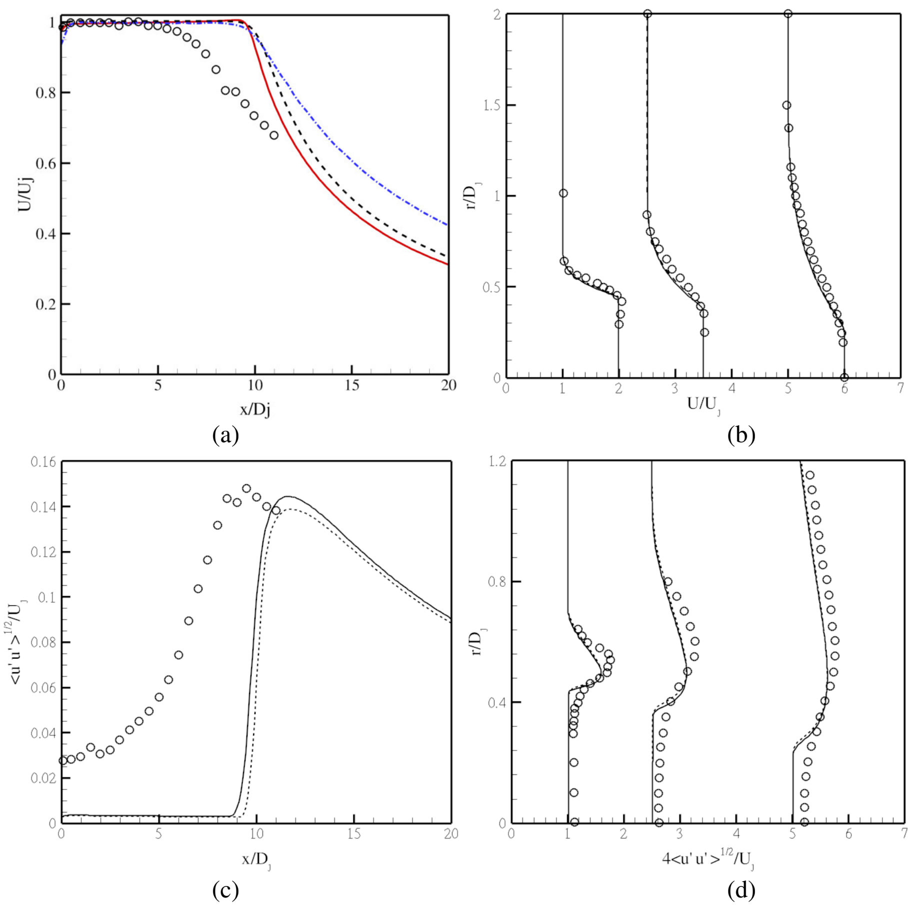

Figure 9. (a) Centerline velocity distribution; (b) Radial profiles of axial velocity; (c) Centerline $\langle u'u' \rangle^{1/2}/U_j$ distribution; (d) Radial profiles of $\langle u'u' \rangle^{1/2}/U_j$ at the axial positions x/Dj = 1.0, x/Dj = 2.5 and x/Dj = 5.0 : '–' corresponds to 2D axissymmetric result, '- -' corresponds to 3D result, '–·–' corresponds to ALMEIDA [2] result and 'o' to experimental results.

Once validated the numerical model, an intermediary step was considered towards the prediction of the flow dynamics of a single interacting with a flat plate. This approach is briefly presented in the next subsection.

3.2. 2D planar results with and without flat plate

Some results for a simple test performed with a 2D planar domain were obtained from the jet-plate interaction simulations. Streamlines originating from the mesh boundaries is presented Figure 10 for jet-plate interaction. They illustrate the entrainment of the surrounding fluid in the jet, and demonstrate that the boundary conditions are appropriate for the incoming fluid into the computational domain in both simulations. The streamlines are fairly parallel to the jet near the inflow, but more perpendicular to the flow direction as the axial distance increases and as the jet becomes "turbulent".

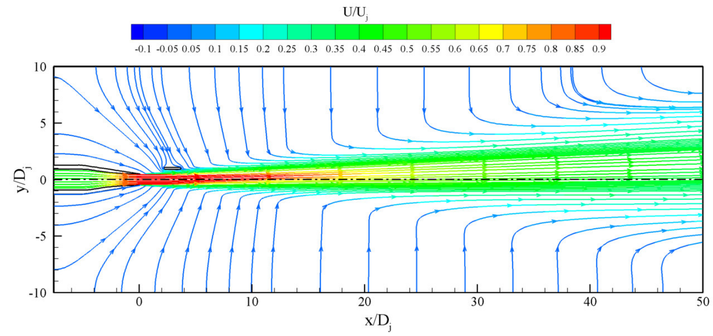

Figure 10. Jet entrainment – Single Jet with Flat Plate.
The streamlines are coloured by U/U_j.

In order to verify the aerodynamics changes induced by the presence of a small flat plate inserted close to the jet exhaust, several Mach number and turbulent kinetic energy perpendicular profiles were plotted along the *x* direction, as can be seen in Figures 11 and 12, respectively. The profiles taken from the single jet baseline case were plotted against the ones obtained from the jet-plate simulation. When the cases are compared, it is possible to note that as *x* increase the Mach number and Turbulent Kinetic Energy (TKE) profiles become slightly different. As expected, for the single jet simulation all profiles keep the symmetry about *x* direction while the profiles for jet-interaction bent upward.

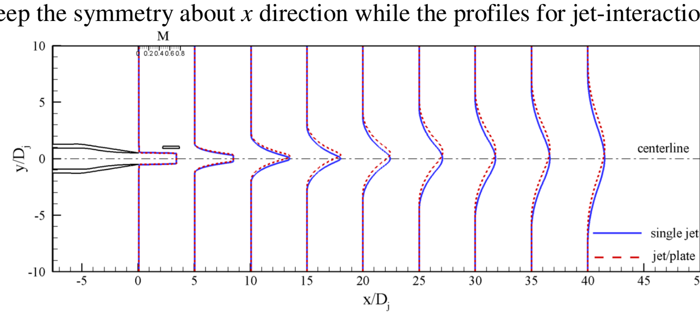

Figure 11 - Mach number profiles vs. *y* coordinate along the *x* direction.

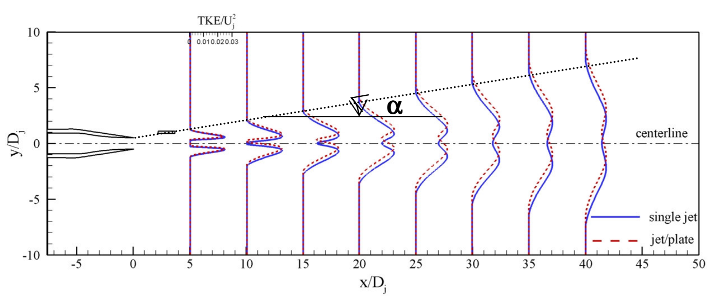

Figure 12 - Turbulent Kinetic Energy Profiles vs *y* coordinate along the *x* direction.

It is noticeable in Figures 11 and 12 that the presence of the small flat plate promotes a weak interaction with the shear layer. Nevertheless, the jet-plate interaction yields a clear modification of the aerodynamic field downstream of the flat plate. It can be easily seen in both figures that the jet flow bents upward after the interaction between the flat plate and the shear layer. This effect can quantitatively be observed taking into account the jet deflection angle, which is the angle between the centerline and the upper limit of the shear layer. Table 2 presents the deflection angle obtained from single jet and jet-plate interaction flow simulations.

Table 2 – Deflection angle.

	Single jet	**Jet-plate**
α	10º	13º

This was a simple test performed to check numerical parameters. A much more detailed analysis must be undertaken in order to completely understand the flow dynamics associated with the jet interacting with a flat plate. It is also important to verify the tridimensional effects associated to this problem. The effects of the parameters L and H (length related to the jet nozzle exit and height of the plate position) seems to play a crucial role in the flow dynamics and consequently in the acoustic signature and must also be entirely evaluated.

3.3. Single jet interacting with a flat plate – 3D

In this section there will be presented the 3D results obtained from the jet-plate interaction and single jet flow simulations. Both cases operating with the same jet exhaust conditions. The fundamental differences between each case will be shown by means of different plots. The most fundamental aspects of the jet exhausting into a quiescent media were qualitatively captured in both simulations. It is possible to observe the formation of the high velocity potential core and the approximately linear spreading in *y* e *x* direction for single jet and jet-plate interaction simulations, as can be seen, for instance, by means of isovalues plots of U/U_j in Figure 13(a) and 13(b), respectively. The distribution of the turbulent kinetic energy TKE/U_j^2 along the shear layers of both single jet and jet-plate interaction flow simulations can be seen in Figures 14(a) and 14(b), respectively.

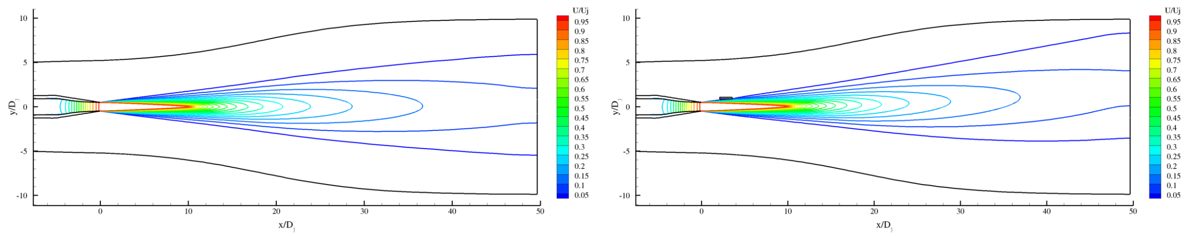

(a) (b)

Figure 13 - Snapshot of isovalues of U/U_j for: (a) single jet; (b) jet-plate interaction.

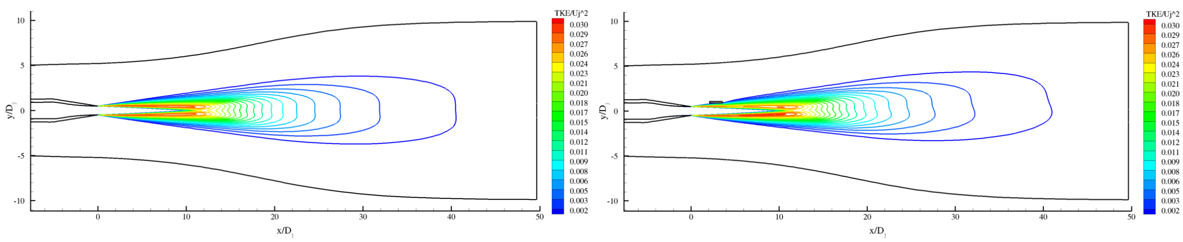

(a) (b)

Figure 14 - Snapshot of isovalues of TKE/U_j^2 for: (a) single jet; (b) jet-plate interaction.

It is noticeable in Figures 13 and 14 that the presence of the small flat plate promotes a weak interaction with the shear layer. Nevertheless, the jet-plate interaction yields a clear modification of the aerodynamic field downstream of the flat plate. It can be easily seen in Figures 13(b) and 14(b) that the jet flow bents upward after the interaction between the flat plate and the shear layer.

It is also possible to note that the presence of the flat plate weakly modify the magnitude of the axial velocity and the turbulent kinetic energy inside the jet flow, as can be seen in Figures 15 - 17.

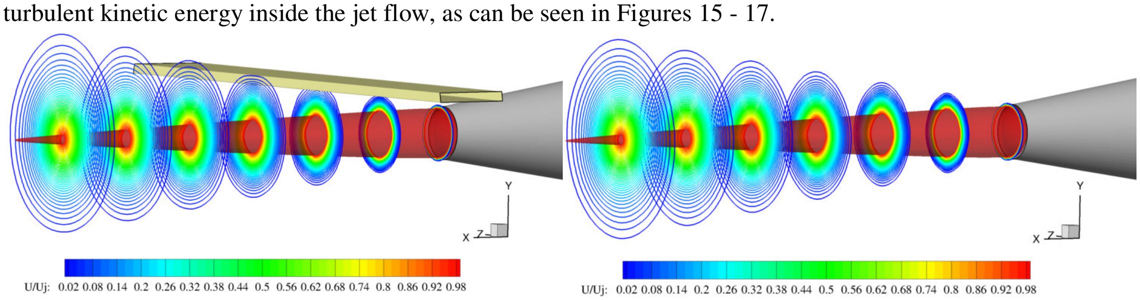

Figure 15. Axial velocity field at planes extracted along axis direction near jet-exit/plate region.

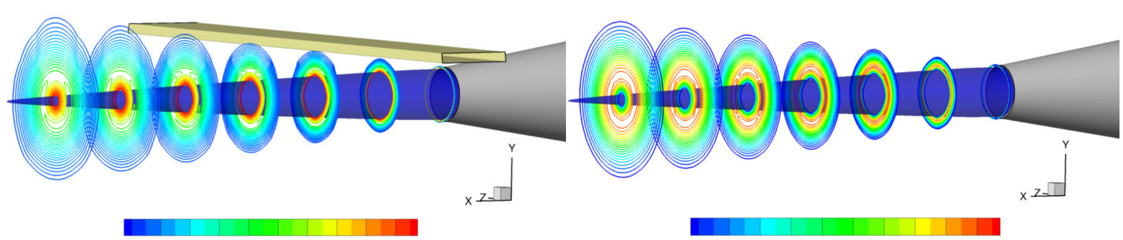

Figure 16. TKE field at planes extracted along axis direction near jet-exit/plate.

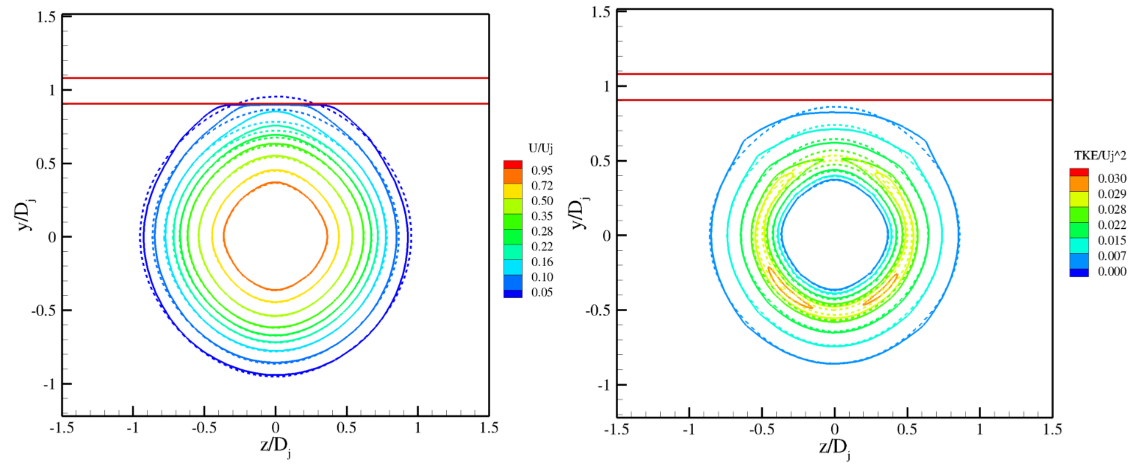

Figure 17. Isovalues of U/U_j, left, and isovalues of TKE, right, at the plane zy across the flat plate. The red parallel lines indicate the presence of the plate. (-) Solid line: jet vs plate; (-.-) Single jet.

The next results will be the distribution of velocity and turbulent kinetic energy (TKE) along the centerline and lipline of the jet – Figure 18.

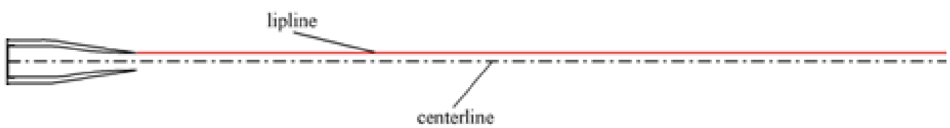

Figure 18 - Position of the centerline and lipline profiles.

Figure 19(a) shows that the distribution of the axial velocity along the centerline is slightly affected by the presence of the plate; consequently it is possible to observe a weak modification of the potential core length. When the attention is focused to the lipline profile, it is possible to see that the velocity increase due the presence of the flat plate, causing an acceleration of the flow in that region.

Figure 19(b) illustrates the turbulent kinetic energy distribution at the jet centreline and lipline respectively. The most important observation is that related to a decrease in the levels of TKE in the lipline for the jet-plate interaction. When looking to the flowfield it is possible to affirm that, locally, the presence of the flat plate promotes a weak interaction in the flow structures close to the nozzle (around 4 D_j). At the jet centreline, the effect is a slightly increase in TKE maintaining the position of the peak levels unchanged.

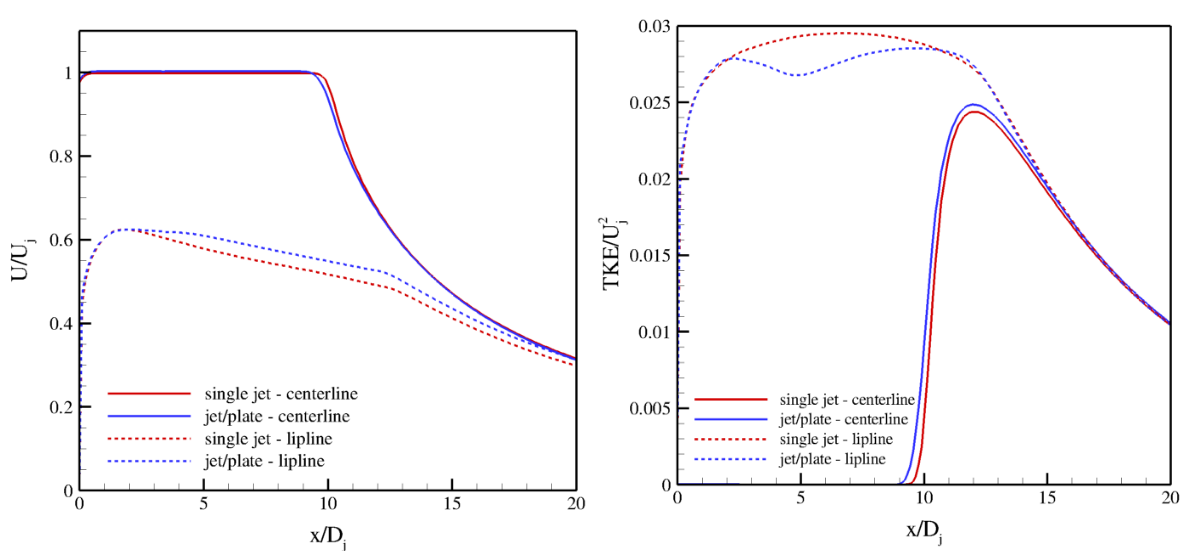

(a) (b)

Figure 19 - Axial velocity (a) and TKE (b) distributions at centerline and lipline.
Comparison with the 3D single jet – *baseline*.

4. CONCLUSIONS

This work presented a currently ongoing research in the Aeroacoustic Group at Federal University of Uberlândia, in order to understand the fluiddynamics and aeroacoustics phenomena involved in the interaction of subsonic jets with surfaces immersed into the flow. Such research activites are part of the "Aeronave Silenciosa" Project under the grant FAPESP 06/52568-7.

The numerical results presented herein were part of a preliminary effort to test different numerical methodologies, numerical parameters like mesh refinement and boundary conditions. The decision made was to give a step back in terms of approaching the problem, considering parametric examples and by doing sets of simple tests to check that parameters. It seems that such strategy has given profits in terms of understanding the whole problem and its limitations and particularities. Moreover, the predicted numerical results were not so far from the experimental data available which brings the information that such approach is working properly. Obviously, a much more detailed analysis must be performed in order to completely understand the flow dynamics associated with the jet interacting with a flat plate. The effects of the parameters L and H (length related to the jet nozzle exit and height of the plate position) seems to play a crucial role in the flow dynamics and consequently in the acoustic signature and must also be entirely evaluated. All these steps are under study and compose the following actions to be undertaken during the realization of this work within the Aeronave Silenciosa Project. The next main step is to incorporate the aeroacoustic model and run the case of a jet interacting with the flate plate in a parametric standpoint.

5. REFERENCES

[1] Oliveira, G. L., Trapp, L. G., Puppin-Macedo, A., Integration Methodology for Regional Jet Aircraft with Underwing Engines, 41st Aerospace Sciences Meeting & Exhibit, 6-9 January, Reno Nevada, 2003.
[2] Almeida, O., Aeroacoustics of Dual-stream Jets with Application to Turbofan Engines, Instituto Tecnológico da Aeronáutica, Tese de Doutorado, 2009.
[3] Way, D. J., and Turner, B. A., "Model Tests Demonstrating Under-Wing Installation Effects on Engine Exhaust Noise," AIAA Paper 80-1048, 1980.
[4] Wang, M. E., "Wing Effect on Jet Noise Propagation," AIAA Paper 80-1047, 1980.
[5] Reddy, N. N., and Tanna, H. K., "Installation Effects on Jet Noise in Flight," AIAA Paper 80-1044, 1980.
[6] Mead, C. J., and Strange, P. J. R., "Under-Wing Installation Effects on Jet Noise at Sideline," AIAA Paper 98-2208, 1998.
[7] Jordan, P. Results from acoustic field measurements. project deliverable D3.6, JEAN-EU. In.: FRAMEWORK PROGRAM, 5., 2002. Proceedings…Poitiers: Laboratoire d'Etude Aerodynamiques. 2002. G4RD-CT-2000-00313
[8] J. G. Shearin, "Investigation of Jet-Installation Noise Sources Under Static Conditions", NASA Technical Paper 2128, August 1983.
[9] Shih, T. H., Lumley, J. L., Zhu, J., "A Realizable Reynolds Stress Albebraic Equation Mode", NASA TM-105993, 1993.
[10] Lien, F. S., Leschziner, M. A., "Low-Reynolds number eddy-viscosity modelling based on non-linear stressstrain/ vorticity relations". In: Rodi, W. and Bergeles, G. (eds), Engineering Turbulence Modelling and Experiments 3, Elsevier, Amsterdam, 1996, pp. 91-100.
[11] Goldberg, U., Batten, P., Palaniswamy, S., Chakravarthy, S., and Peroomiam, O., "Hypersonic Flow Predictions Using Linear and Nonlinear Turbulence Closures", Journal of Aircraft, Vol 37, No. 4, 2000, pp. 671-675.

6. RESPONSIBILITY NOTICE

The authors are the only responsible for the printed material included in this paper.